Phonon-dependent transport through a serially coupled double quantum dot system

M. Bagheri Tagani and H. Rahimpour Soleimani†

Department of Physics, University of Guilan, P. O. Box 41335-1914, *Rasht, Iran*

(Received 14 October 2013; revised manuscript received 28 November 2013; published online 25 March 2014)

Using Keldysh nonequilibrium Green function formalism and mapping a many-body electron–phonon interaction onto a one body problem, the electron transport through a serially coupled double quantum dot system is analyzed. The influence of the electron–phonon interaction, temperature, detuning, and interdot tunneling on the transmission coefficient and current is studied. Our results show that the electron–phonon interaction results in the appearance of the side peaks in the transmission coefficient, whose height is strongly dependent on the phonon temperature. We have also found that the inequality of the electron–phonon interaction strength in two dots gives rise to an asymmetry in the current–voltage characteristic. In addition, the temperature difference between the phonon and electron subsystems results in the reduction of the saturated current and the destruction of the step-like behavior of the current. It is also observed that the detuning can improve the magnitude of the current by compensating the mismatch of the quantum dots energy levels induced by the electron–phonon interaction.

Keywords: quantum dot, electron–phonon interaction, Keldysh nonequilibrium Green function formalism, current–voltage characteristic

PACS: 73.23.Hk, 73.63.Kv **DOI:** 10.1088/1674-1056/23/5/057302

1. Introduction

Study of transport through quantum dot-based devices has attracted a lot of attention, both experimentally and theoretically.[1–16] One of the most interesting devices is composed of two serial or parallel quantum dots (DQD) because of their molecular-like behavior. The discreteness of the energy levels, strong electron correlations, interference effect, and so on result in the novel and interesting phenomena in the electron transport through DQDs, such as: Coulomb and spin blockade effects,[8,17–20] Kondo effect,[14,21–24] ratchet effect,[25] negative differential conductance (NDC),[26,27] etc. In addition, the DQD systems are promising candidates for spintronic applications.[28]

The electron–phonon interaction (EPI) in mesoscopic systems is a very interesting issue that has been extensively addressed in the last two decades.[4,8,29–43] The EPI significantly influence the electron transport through QDs and molecules. Coupling of the center-of-mass motion of the molecule and electron hoping,[29] and thermally induced acoustic phonons[44] are the main origin of the coupling between the electronic and vibrational degrees of freedom. The EPI in single QD devices has been widely studied, from both experimental and theoretical point of views. The master equation approach[30,32,33] and the Keldysh nonequilibrium formalism[31,37,42,43,45,46] have been used to investigate the effect of the EPI on the current and conductance. The results show that the EPI results in the NDC,[4,32,41] appearance of the sidebands in the density of the state spectrum,[45,46] phonon-assisted peaks in the conductance,[31,42] and so on. However, the influence of the EPI on the transport properties of the DQD system is a very interesting issue which needs more research.

In this article, we analyze the electron transport through a DQD system by taking into account the EPI. We assume that the electron of each dot interacts with a dispersionless optical phonon mode. Using the Keldysh nonequilibrium Green function formalism and nonperturbative scheme proposed by Bonča and co-workers,[47] the current and transmission coefficient are analyzed as a function of temperature, energy levels of the QD, and EPI strength. Unlike rate equation formalism, this scheme is valid for strong EPI and explains the quantum coherence effects. Bonça's scheme allows us to convert a many-body problem into a one-body problem. Here, we assume that there are a lot of channels for the transport of the electron inside each dot. The number of channels is equal to the phonon number. The electron can change its phononic channel in the QD due to the electron–phonon interaction. Using the mentioned scheme, the electron–phonon interaction term is eliminated from the Hamiltonian of the whole system and, as a result, the problem becomes analytically solvable. The same problem was investigated in Ref. [43] with concentration on the shot noise of the system. We have also considered the influence of the temperature difference between the phononic and electronic subsystems on the transport properties of the system. The phonon temperature can be more than the electron's temperature because of the smaller heat capacity of phonon subsystems. This difference can result in several interesting phenomena, such as the appearance of the absorp-

†Corresponding author. E-mail: rahimpour@guilan.ac.ir

© 2014 Chinese Physical Society and IOP Publishing Ltd

tion sidebands for increasing temperatures.[48,49] Furthermore, the influence of the inequality of the EPI strength in two dots on the transport properties of the system is analyzed. This inequality can significantly affect the current–voltage characteristic of the system. Although the same system was examined in Ref. [43], the influence of the temperature difference of the electron and phonon subsystems, and asymmetric EPI were not considered there. In the next section, the Hamiltonian and formalism used to describe the system are given. Section 3 is devoted to the numerical results, and at the end a summary is given.

2. Model and formalism

We consider a serial DQD system and assume that the electrons of each dot interact with a dispersionless optical phonon mode. The Hamiltonian describing the whole system is given as

$$H = H_{\rm leads} + H_{\rm DQD} + H_{\rm T}, \tag{1}$$

where $H_{\rm leads} = \sum_{\alpha k\sigma} \varepsilon_{\alpha k\sigma} c^{\dagger}_{\alpha k\sigma} c_{\alpha k\sigma}$ describes the leads using the non-interacting quasi particle approximation. $c^{\dagger}_{\alpha k\sigma}$ creates an electron with wave vector k, spin σ, and energy $\varepsilon_{\alpha k\sigma}$ in lead $\alpha = {\rm L}, {\rm R}$. $H_{\rm DQD}$ is given as

$$\begin{aligned} H_{\rm DQD} &= \sum_{i={\rm L,R}} \sum_{\sigma} [\varepsilon_{i\sigma} n_{i\sigma} + \omega_i a^{\dagger}_i a_i + \lambda_i [a^{\dagger}_i + a_i] n_{i\sigma}] \\ &\quad + \sum_{\sigma} t [d^{\dagger}_{L\sigma} d_{R\sigma} + d^{\dagger}_{R\sigma} d_{L\sigma}], \end{aligned} \tag{2}$$

where $d^{\dagger}_{i\sigma}$ is the creation operator in the ith dot, $n_{i\sigma} = d^{\dagger}_{i\sigma} d_{i\sigma}$ is the occupation number, $\varepsilon_{i\sigma}$ denotes the energy level of the ith dot, and we assume $\varepsilon_{{\rm R}\sigma} = \varepsilon_{{\rm L}\sigma} + \Delta$, where Δ stands for the detuning. The a_i is the phonon annihilation operator, while λ_i describes the coupling of the electronic and phononic degrees of freedom. The t describes the interdot tunneling assumed to be spin-independent. It is assumed that each QD can have up to one electron because the one-site Coulomb interaction is order of a few meV and, as a result, the population of the QD can be easily controlled using a gate voltage in experiments. The tunneling between the QDs and the leads is described by $H_{\rm T}$

$$H_{\rm T} = \sum_{k\sigma} [V_{{\rm L}k\sigma} c^{\dagger}_{{\rm L}k\sigma} d_{{\rm L}\sigma} + V_{{\rm R}k\sigma} c^{\dagger}_{{\rm R}k\sigma} d_{{\rm R}\sigma} + {\rm h.c}], \tag{3}$$

where $V_{\alpha k\sigma}$ is the tunneling matrix element.

Equation (2) describes a many-body problem involving the phonon absorption and emission when the electron tunnels to the QD. We can map the problem to a one-body problem by means of the method introduced by Bonča and co-workers.[47] Each QD can have one electron and n phonons; thus, a polaron eigenstate can be used to describe the state of each dot[31,43]

$$|i\sigma, n\rangle = d^{\dagger}_{i\sigma} \frac{(a^{\dagger}_i)^n}{\sqrt{n!}} |0\rangle, \quad n \geq 0, \tag{4}$$

where $|0\rangle$ is the vacuum state. Note that because the electrodes are normal metals and no magnetic field is applied, the spin index will be omitted in the following. Using the above transformation, $H_{\rm DQD}$ is written as

$$\begin{aligned} H_{\rm DQD} &= \sum_{i={\rm L,R}, n\geq 0} \{\varepsilon_{in} |i,n\rangle\langle i,n| + \lambda\sqrt{n+1} (|i,n+1\rangle\langle i,n| \\ &\quad + |i,n\rangle\langle i,n+1|)\} + \sum_{n\geq 0} t [|L,n\rangle\langle R,n| + |R,n\rangle\langle L,n|], \end{aligned} \tag{5}$$

where $\varepsilon_{in} = \varepsilon_{i\sigma} + n\omega_i$. Because of the transformation, $H_{\rm leads}$ and $H_{\rm T}$ become

$$H_{\rm leads} = \sum_{\alpha kn} \varepsilon_{\alpha kn} |\alpha kn\rangle\langle \alpha kn|, \tag{6a}$$

$$H_{\rm T} = \sum_{kn} [V_{{\rm L}k} |Lkn\rangle\langle Ln| + V_{{\rm R}k} |Rkn\rangle\langle Rn| + {\rm h.c}], \tag{6b}$$

where $\varepsilon_{\alpha kn} = \varepsilon_{\alpha k\sigma} + n\omega_\alpha$, and $|\alpha k\rangle$ denotes an electron state with wave vector k in lead α. Indeed, there are various channels for the transport of the electron through the system and the number of the channels is equal to the number of phonons. The phonon population is conserved in the tunneling from the leads to the QDs, or from one QD to the other, because the tunneling is assumed to be an elastic process. On the other hand, the electron of the QD can change transport channel by absorbing or emitting a phonon. The probability of being in the nth channel is given by a weight factor, $P_{in} = {\rm e}^{-n\omega_i/kT_{\rm ph}} (1 - {\rm e}^{-\omega_i/kT_{\rm ph}})$ where $T_{\rm ph}$ denotes the phonon temperature. Because the heat capacity of phonon subsystem is smaller than the electron subsystem, the phonons can have a higher temperature than the electron's temperature. Such a difference can result in the appearance of absorption sidebands as temperatures increase in the carbon nanotube QDs.[48,49]

Now, we define the Dirac brackets as operators:[31]

$$d^{\dagger}_{\alpha n} \equiv |\alpha n\rangle, \quad c^{\dagger}_{\alpha kn} \equiv |\alpha kn\rangle, \tag{7}$$

thus, equations (5) and (6) are mapped in the operator representation as

$$\begin{aligned} H &= \sum_{\alpha kn} \varepsilon_{\alpha kn} c^{\dagger}_{\alpha kn} c_{\alpha kn} \\ &\quad + \sum_{\alpha n} \{\varepsilon_{\alpha n} n_{\alpha n} + \lambda\sqrt{n+1} [d^{\dagger}_{\alpha n+1} d_{\alpha n} + d^{\dagger}_{\alpha n} d_{\alpha n+1}]\} \\ &\quad + t \sum_{n} \{d^{\dagger}_{{\rm L}n} d_{{\rm R}n} + d^{\dagger}_{{\rm R}n} d_{{\rm L}n}\} \\ &\quad + \sum_{kn} \{V_{{\rm L}k} c^{\dagger}_{{\rm L}kn} d_{{\rm L}n} + V_{{\rm R}k} c^{\dagger}_{{\rm R}kn} d_{{\rm R}n} + {\rm h.c}\}, \end{aligned} \tag{8}$$

where these operators satisfy the anticommunication relations as

$$\{d_{\alpha n}, d^{\dagger}_{\alpha' m}\} = \delta_{\alpha\alpha'} \delta_{nm}, \quad \{c_{\alpha kn}, c^{\dagger}_{\alpha' k' m}\} = \delta_{\alpha\alpha'} \delta_{kk'} \delta_{nm}. \tag{9}$$

The electronic current crossing from the nth channel and the lead α is given as

$$I_{\alpha n}(t) = -e \left\langle \frac{\rm d}{{\rm d}t} N_{\alpha n} \right\rangle = \frac{-{\rm i}e}{\hbar} \langle [H, N_{\alpha n}] \rangle, \tag{10}$$

where $N_{\alpha n} = \sum_k c^{\dagger}_{\alpha kn} c_{\alpha kn}$. With respect to Eqs. (8) and (9), we

have

$$I_{\alpha n}(t)=\frac{e}{\hbar}\sum_k[V_{\alpha k}G^<_{\alpha n,\alpha k n}(t,t)-V^*_{\alpha k}G^<_{\alpha k n,\alpha n}(t,t)], \quad (11)$$

where the lesser Green functions are defined as: $G^<_{\alpha n,\alpha k n}(t,t')=i\langle c^\dagger_{\alpha k n}(t')d_{\alpha n}(t)\rangle$, and $G^<_{\alpha k n,\alpha n}(t,t')=i\langle d^\dagger_{\alpha n}(t')c_{\alpha k n}(t)\rangle$. To compute the Green functions presented in Eq. (11), the equation of motion technique within the Keldysh nonequilibrium Green function formalism is used.[50] Using the Langreth continuation theorem,[51] it is straightforward to show that

$$G^<_{\alpha n,\alpha k n}(t,t')=V^*_{\alpha k}\int \mathrm{d}t_1[G^{\mathrm{r}}_{\alpha n,\alpha n}(t,t_1)g^<_{\alpha k n}(t_1,t)+G^<_{\alpha n,\alpha n}(t,t_1)g^a_{\alpha k n}(t_1,t)], \quad (12a)$$

$$G^<_{\alpha k n,\alpha n}(t,t')=V_{\alpha k}\int \mathrm{d}t_1[g^{\mathrm{r}}_{\alpha k n}(t,t_1)G^<_{\alpha n,\alpha n}(t_1,t)+g^<_{\alpha k n}(t,t_1)G^a_{\alpha n,\alpha n}(t_1,t)], \quad (12b)$$

where $g^{\mathrm{r(a)}}_{\alpha k n}(t,t')=\mp\mathrm{i}\Theta(\pm t\mp t')\langle\{c_{\alpha k n}(t),c^\dagger_{\alpha k n}(t')\}\rangle$ is the retarded (advanced) Green function of the isolated electrode, whereas $G^{\mathrm{r(a)}}_{\alpha n,\alpha m}=\mp\mathrm{i}\Theta(\pm t\mp t')\langle\{d_{\alpha n}(t),d^\dagger_{\alpha m}(t')\}\rangle$ stands for the retarded (advanced) Green function of the αth dot in the presence of the couplings. Using the identity, $G^{\mathrm{r}}-G^a=G^>-G^<$, equation (11) becomes

$$I_{\alpha n}=\frac{e}{\hbar}\sum_k|V_{kn}|^2\int \mathrm{d}t_1[G^>_{\alpha,\alpha n}(t,t_1)g^<_{\alpha k n}(t_1,t)-g^>_{\alpha k n}(t,t_1)G^<_{\alpha n,\alpha n}(t_1,t)]. \quad (13)$$

Using the wide band approximation in which the lead-dot coupling is assumed to be energy-independent and setting the unperturbed Green functions of the leads in Eq. (12), the current is given by

$$I_{\alpha n}=\frac{\mathrm{i}e}{h}\Gamma_\alpha\int \mathrm{d}\varepsilon[f^n_\alpha(\varepsilon)G^>_{\alpha n,\alpha n}(\varepsilon)+(1-f^n_\alpha(\varepsilon))G^<_{\alpha n,\alpha n}(\varepsilon)], \quad (14)$$

where $\Gamma_\alpha=2\pi\sum_k|V_{\alpha k}|^2$ is the coupling strength between the αth dot and lead, and $f^n_\alpha(\varepsilon)=(1+\exp((\varepsilon-n\omega_\alpha-\mu_\alpha)/kT))^{-1}$ is the Fermi distribution function of the lead α and $\mu_\alpha=E_{\mathrm{f}}\pm V/2$ (a plus sign for the left lead and a negative sign for the right lead). In order to compute the Green function of the system, the equation of motion technique is used, so that the retarded Green functions obey the following matrix equation

$$[\varepsilon-\varepsilon_{\alpha m}+i/2\Gamma_\alpha]G^{\mathrm{r}}_{\alpha m,\beta n}(\varepsilon)=\delta_{\alpha\beta}\delta_{mn}+\lambda_\alpha\sqrt{m+1}G^{\mathrm{r}}_{\alpha m+1,\beta n}(\varepsilon)+\lambda_\alpha\sqrt{m}G^{\mathrm{r}}_{\alpha m-1,\beta n}(\varepsilon)+tG^{\mathrm{r}}_{\alpha' m,\beta n}(\varepsilon), \quad (15)$$

where $\alpha'=R(L)$ is opposite of $\alpha=L(R)$. Now, one can easily compute the retarded Green function in the matrix form as

$$G^{\mathrm{r}}_{\alpha m,\alpha n}(\varepsilon)=[\boldsymbol{H}_{1\alpha}(\varepsilon)-\boldsymbol{H}_2(\boldsymbol{H}_{3\alpha}(\varepsilon))^{-1}\boldsymbol{H}_2]^{-1}_{mn}, \quad (16a)$$

$$G^{\mathrm{r}}_{\alpha m,\alpha' n}(\varepsilon)=[(\boldsymbol{H}_{3\alpha'}(\varepsilon))^{-1}\boldsymbol{H}_2G^{\mathrm{r}}_{\alpha',\alpha'}(\varepsilon)]_{mn}, \quad (16b)$$

where the matrices presented in the above equations have a size equal to the number of phonons and are given as

$$\boldsymbol{H}_{1\alpha}(\varepsilon)=\begin{pmatrix}\varepsilon-\varepsilon_{\alpha0}+\mathrm{i}/2\Gamma_\alpha & -\lambda_\alpha & 0 & 0 & \dots\\ -\lambda_\alpha & \varepsilon-\varepsilon_{\alpha1}+\mathrm{i}/2\Gamma_\alpha & -\sqrt{2}\lambda_\alpha & 0 & \dots\\ 0 & -\sqrt{2}\lambda_\alpha & \varepsilon-\varepsilon_{\alpha2}+\mathrm{i}/2\Gamma_\alpha & -\sqrt{3}\lambda_\alpha & \dots\\ \dots & \dots & \dots & \dots & \dots\\ \dots & \dots & \dots & \dots & \dots\end{pmatrix}, \quad (17)$$

$$\boldsymbol{H}_2=\begin{pmatrix}t & 0 & \dots\\ 0 & t & \dots\\ \dots & \dots & t\end{pmatrix}, \quad (18)$$

$$\boldsymbol{H}_{3\alpha}(\varepsilon)=\begin{pmatrix}\varepsilon-\varepsilon_{\alpha'0}+\mathrm{i}/2\Gamma_{\alpha'} & -\lambda_{\alpha'} & 0 & 0 & \dots\\ -\lambda_{\alpha'} & \varepsilon-\varepsilon_{\alpha'1}+\mathrm{i}/2\Gamma_{\alpha'} & -\sqrt{2}\lambda_{\alpha'} & 0 & \dots\\ 0 & -\sqrt{2}\lambda_{\alpha'} & \varepsilon-\varepsilon_{\alpha'2}+\mathrm{i}/2\Gamma_{\alpha'} & -\sqrt{3}\lambda_{\alpha'} & \dots\\ \dots & \dots & \dots & \dots & \dots\\ \dots & \dots & \dots & \dots & \dots\end{pmatrix}. \quad (19)$$

$G^{<(>)}(\varepsilon)$ is computed by using the Keldysh Green function technique as $G^{<(>)}=G^{\mathrm{r}}\Sigma^{<(>)}G^a$, where the self-energies are given as $\Sigma^{<(>)}(\varepsilon)_{n,n}=\pm\sum_\alpha\Gamma_\alpha f^{n+(-)}_\alpha(\varepsilon)$, where $f^{n-}_\alpha=1-f^n_\alpha$. Indeed, because the correlated Hamiltonian, Eq. (1), is mapped to a one-body problem, Eq. (8), the tunneling is considered as an elastic process and the QDs are serially coupled to the leads, and the self-energy matrices are diagonal and proportional to the tunneling. Therefore, one can easily obtain the following equation for the lesser (greater) Green function

$$G^{<(>)}_{\alpha n,\alpha n}(\varepsilon)=\pm\mathrm{i}\sum_m[\Gamma_\alpha f^{m+(-)}_\alpha(\varepsilon)|G^{\mathrm{r}}_{\alpha n,\alpha m}(\varepsilon)|^2+\Gamma_{\alpha'}f^{m+(-)}_{\alpha'}(\varepsilon)|G_{\alpha n,\alpha' m}(\varepsilon)|^2]. \quad (20)$$

By substituting Eq. (20) in Eq. (14), and summing on all phonon channels, the final expression of the current crossing from the lead α is given by

$$I_\alpha=\frac{e}{h}\Gamma_\alpha\sum_{n,m}\int \mathrm{d}\varepsilon\Big\{P_nf^n_\alpha(\varepsilon)\sum_{\beta=L,R}[\Gamma_\beta|G^{\mathrm{r}}_{\alpha n,\beta m}(\varepsilon)|^2$$

$$\times(1-f_\beta^m(\varepsilon))\big]-P_m(1-f_\alpha^n(\varepsilon))$$
$$\times\sum_{\beta=L,R}\big[\Gamma_\beta|G^{\rm r}_{\alpha n,\beta m}(\varepsilon)|^2 f_\beta^m(\varepsilon)\big]\Big\}. \quad (21)$$

Now, we define the transmission coefficient as $T(\varepsilon)=\mathrm{trace}(\Gamma_{\rm L}G^{\rm r}(\varepsilon)\Gamma_{\rm R}G^{a}(\varepsilon))$ which is given as follows:

$$T_{\rm el}(\varepsilon) = \sum_n \Gamma_{\rm L}\Gamma_{\rm R}|G^{\rm r}_{{\rm LR}}(\varepsilon)|^2_{nn}, \quad (22a)$$
$$T(\varepsilon) = \sum_{nm} P_n\Gamma_{\rm L}\Gamma_{\rm R}|G^{\rm r}_{{\rm LR}}|^2_{nm}, \quad (22b)$$

where $T_{\rm el}$ is the elastic contribution to the transport, so that the phonon population is conserved during the transport, whereas T describes the total transmission coefficient. For simulation purposes, we set the phonon energy as the energy unit.

3. Results and discussion

Figure 1 describes the elastic and total transmission coefficients as a function of energy for both EP equilibrium and EP nonequilibrium. In the absence of the EPI, $T_{\rm el}$ and $T_{\rm tot}$ are identical and show two peaks located in the bonding state, $\varepsilon=\varepsilon_{\rm L}-t$, and antibonding state, $\varepsilon=\varepsilon_{\rm L}+t$. In the presence of the EPI, the height of the peaks decreases, whereas the number of peaks significantly increases. First, we analyze the EP equilibrium case. The position of the peaks is changed due to the polaronic shift. Furthermore, $T_{\rm el}$ is no longer identical to $T_{\rm tot}$. One can observe the phonon-assisted peaks whose distance from the main peaks is equal to $n\omega$ where n is an integer. Although the height of the side peaks is low in $T_{\rm el}$, $T_{\rm tot}$ exhibits higher peaks, indicating that the inelastic transport is dominant. When the EPI is present in both dots, the distance between main peaks increases; however, the height of the peaks of $T_{\rm el}$ reduces, which shows that a higher portion of the transport is due to inelastic processes. Therefore, the height of the phonon-assisted peaks is significantly increased. In the case of the EP nonequilibrium, the phonon temperature is comparable with the phonon energy, so more phonons are in the system and, as a consequence, the transmission coefficient shows more peaks. For $T_{\rm el}$, the height of the peaks reduces while their number increases, which shows that the phonon channels have a more significant role in the transport. It is also observed that, although the height of the main peaks of $T_{\rm tot}$ reduces in the EP nonequilibrium, the height of the phonon-assisted peaks increases.

To analyze the influence of the EPI in more detail, we define the local density of the states (LDS) as $A_{\alpha,\alpha}=-2\mathrm{Im}\{\mathrm{tr}(G^{\rm r}_{\alpha,\alpha}(\varepsilon))\}$ containing important information about the QD–lead couplings, QD–QD coupling, and EPI. As one expects, $A_{\alpha,\alpha}$ shows two main peaks in the bonding and antibonding states when $\lambda_i=0$. The behavior of the LDS is very interesting when the EPI is just in one dot, the left dot. In this case, $A_{\rm LL}$ and $A_{\rm RR}$ have different behaviors. $A_{\rm LL}$ exhibits two main peaks in the bonding and antibonding states. In the EP nonequilibrium there are extra peaks due to the phonon emission and absorption. Unlike $A_{\rm LL}$, $A_{\rm RR}$ has three main peaks and the third one is located in the resonance energy, $\varepsilon=\varepsilon_{\rm R}$. This peak is only observed in the EP nonequilibrium for $A_{\rm LL}$ with low height. Note that, when $\lambda_{\rm R}=0$, there is a detuning in the QDs' energy levels, resulting in an asymmetry. An increase of phonon temperature results in the appearance of side peaks in $A_{\rm RR}$. When $\lambda_{\rm L}=\lambda_{\rm R}$ $A_{\rm LL}$ and $A_{\rm RR}$ behave in the same manner, so that main peaks are located in the bonding and antibonding states. It is clear that the height of the side peaks is controlled by the EPI's strength because the probability of the phonon participation in the transport is enhanced by an increase of λ_i.

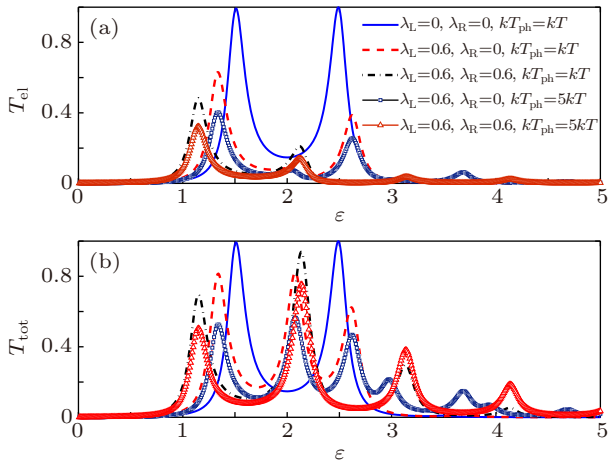


Fig. 1. (color online) (a) Elastic and (b) total transmission coefficients as a function of energy. The parameters are $\Gamma_{\rm L}=\Gamma_{\rm R}=0.2$, $kT=0.2$, $t=0.5$, and $\varepsilon_{\rm L}=\varepsilon_{\rm R}=2$.

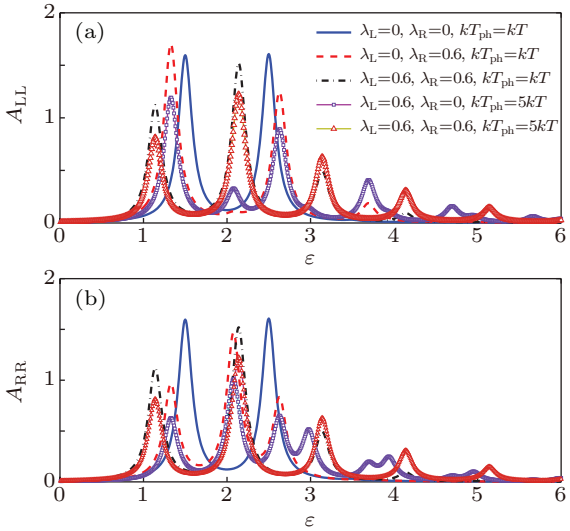


Fig. 2. (color online) (a) $A_{\rm LL}$ and (b) $A_{\rm RR}$ as a function of energy. The parameters are the same as Fig. 1.

Current–voltage characteristic is plotted in Fig. 3. In the case of $\lambda_\alpha=0$, elastic transport, the current exhibits three steps, indicating the empty and full states. When $|V|<\varepsilon_{\alpha\sigma}-t$, low bias regime, the system is empty and the current is zero. With an increase of voltage, the current monotonically increases until the system becomes a fully occupied, high bias

regime and, as a result, the current will be saturated. Asymmetry in the EPI results in the asymmetry of the current–voltage characteristic. The results show that the saturated current is higher when the QD with weaker λ acts as an emitter. EP nonequilibrium gives rise to the destruction of the steps and the decrease of the saturated current magnitude. When the EPI strength is the same in both dots, the current–voltage characteristic is symmetric. In this case, the results are in good agreement with results presented in Ref. [42]. The EP nonequilibrium results in the reduction of the width and height of the steps.

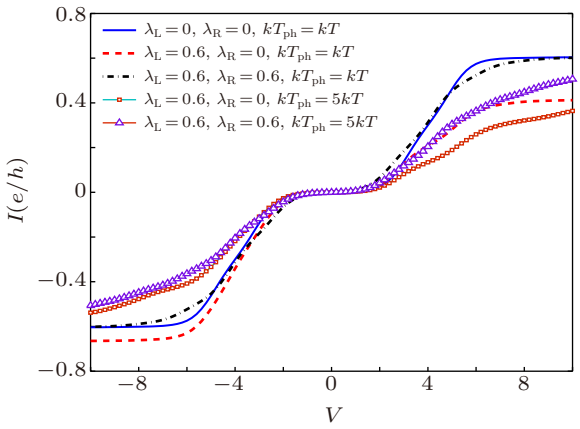


Fig. 3. (color online) Current versus voltage. The parameters are the same as Fig. 1.

Electrical conductance, $\mathrm{d}I/\mathrm{d}V$, is shown in Fig. 4 as a function of bias. Electrical conductance can reveal information that is not well seen in the current–voltage characteristic. In the elastic transport, the conductance has two main peaks because the system can have up to two electrons. The EPI results in the shift of the main peaks and the appearance of the extra peaks. In the case of $\lambda_L \neq \lambda_R$, the conductance spectrum is sensitive to the sign of the voltage, so that it has two distinct peaks when the left lead is an emitter, while the peaks are merged when the right lead is an emitter. This leads to an asymmetry in the conductance spectrum. Furthermore, the height of the peaks is significantly reduced. In the case of

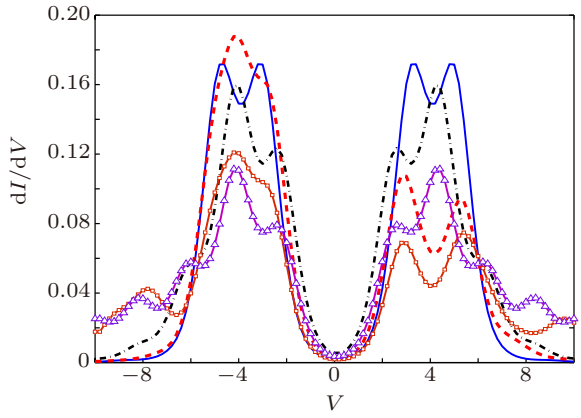


Fig. 4. (color online) Electrical conductance, $\mathrm{d}I/\mathrm{d}V$ against voltage. The parameters are the same as Fig. 1.

the EP nonequilibrium, the conductance shows a more complicated behavior. The number of peaks significantly increases because the phonons have a more colorful role in the transport. Furthermore, the height of the main peaks is reduced, whereas the height of the phonon-assisted peaks is increased.

The influence of the detuning, $\varepsilon_{R\sigma} = \varepsilon_{L\sigma} + \Delta$, and ratio of λ_R to λ_L is analyzed in Fig. 5(a). It is obvious that the detuning results in the reduction of the current because the probability of the electron tunneling between QDs reduces. However, because the EPI strength gives rise to the renormalization of the QDs energy levels, detuning can sometimes increase the current. We consider the situation in which the left lead acts as an emitter, whereas the right lead is a collector. As one expects, the maximum of the current takes place in $\Delta = 0$, when $\alpha = \lambda_R/\lambda_L = 1$. For $\alpha < 1$, the maximum value of the current is observed in $\Delta = -\lambda_L/\omega(1-\alpha)$, because this detuning compensates for the detuning that has resulted from the EPI. For $\alpha < 1$, and $\Delta > 0$, the current is suppressed because the electron of the left dot cannot tunnel from the left dot to the right one. With an increase of α, the phonons play more important role in the transport in the right dot, so that the highest value of the current is observed in $\alpha > 1$. Our results show that the increase of the EPI in the dot coupled to the collector electrode gives rise to the increase of the current. Figure 5(b) shows the influence of the interdot tunneling and EPI on the current. The interdot tunneling is controlled by using a gate voltage so that both weak and strong times are easily accessible in the experiments. In weak times, the current is suppressed because the interdot tunneling is blocked. Indeed, an electron has to stay in a dot for a long time and, as a result, the next electron cannot tunnel into the dot. The current is significantly increased by an increase of t. In addition, the reduction of the current due to the EPI can be improved by increasing the interdot tunneling strength, so that the current has maximum values in the strong λ and t.

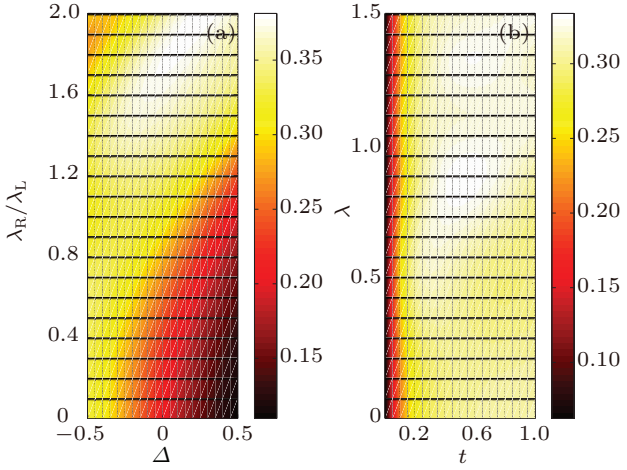


Fig. 5. (color online) Color map of the current. (a) $\lambda_L = 0.6$, $\varepsilon_L = 2$, and (b) $\lambda_L = \lambda_R$. We set $V = 4$, and $T_{ph} = T$ in both figures.

4. Summary

In this article, we have analyzed the electron transport through a serially coupled double quantum dot system while taking into account the electron–phonon interaction (EPI). A nonperturbative shame and the Keldysh nonequilibrium Green function formalism are used to compute the current and transmission coefficients. Our results show that the EPI results in the appearance of side peaks in the transmission coefficient, whose height is dependent on the EPI strength and phonon temperature. In addition, it is found that the temperature difference between the phononic and electronic subsystems gives rise to a reduction of the current and the destruction of its step-like behavior.

References

[1] Van der Wiel W G, De Franceschi S, Elzerman J M, Fujisawa T, Tarucha S and Kouwenhoven L P 2003 *Rev. Mod. Phys.* **75** 1

[2] Hanson R, Kouwenhoven L P, Petta J R, Tarucha S and Vandersypen L M K 2007 *Rev. Mod. Phys.* **79** 1217

[3] Ono K, Austing D G, Tokura Y and Tarucha S 2002 *Science* **297** 1313

[4] LeRoy B J, Lemay S G, Kong J and Dekker C 2004 *Nature* **432** 371

[5] Moldoveanu V, Gudmundsson V and Manolescu A 2007 *Phys. Rev. B* **76** 085330

[6] Kießlich G, Schöll E, Brandes T, Hohls F and Haug R J 2007 *Phys. Rev. Lett.* **99** 206602

[7] Molitor F, Dröscher S, Güttinger J, Jacobsen A, Stampfer C, Ihn T and Ensslin K 2009 *Appl. Phys. Lett.* **94** 222107

[8] Hüttel A K, Witkamp B, Leijnse M, Wegewijs M R and van der Zant H S J 2009 *Phys. Rev. Lett.* **102** 225501

[9] Sánchez R, López R, Sśnchez D and Büttiker M 2010 *Phys. Rev. Lett.* **104** 076801

[10] Weymann I and Barnaś 2010 *Phys. Rev. B* **82** 165450

[11] Koh T S, Simmons C B, Eriksson M A, Coppersmith S N and Friesen M 2011 *Phys. Rev. Lett.* **106** 186801

[12] Gawarecki K and Machnikowski P 2012 *Phys. Rev. B* **85** 041305(R)

[13] Fang Z H, Zhang X G, Chen K J, Qian X Y, Xu J, Huang X F end He F 2010 *Chin. Phys. Lett.* **27** 057304

[14] Chen J F, Wu S Q, Hou T and Zhao G P 2010 *Chin. Phys. Lett.* **27** 047201

[15] Chen B J, Chen X W, Shi Z G and Song K H 2009 *Acta Phys. Sin.* **58** 2720 (in Chinese)

[16] Xu J, Shangguan W Z and Zhan S C 2005 *Chin. Phys.* **14** 2093

[17] Johnson A C, Petta J R and Marcus C M 2005 *Phys. Rev. B* **72** 165308

[18] Liu H W, Fujisawa T, Hayashi T and Hirayama Y 2005 *Phys. Rev. B* **72** 161305

[19] I.narrea J, Platero G and MacDonald A H 2007 *Phys. Rev. B* **76** 085329

[20] Yian W X, Zhang Y P, Wen Y B, Li X P, Xu L P and Gong J P 2010 *Chin. Phys. B* **19** 027302

[21] Sasaki S, Tamura H, Akazaki T and Fujisawa T 2009 *Phys. Rev. Lett.* **103** 266806

[22] Ferreira I L, Orellana P A, Martins G B, Souza F M and Vernek E 2011 *Phys. Rev. B* **84** 205320

[23] Žitko R, Lim J S, López R, Martinek J and Simon P 2012 *Phys. Rev. Lett.* **108** 166605

[24] Lü R and Liu Z R 2007 *Chin. Phys. Lett.* **24** 195

[25] Moldoveanu V and Tanatar B 2010 *Phys. Rev. B* **82** 205312

[26] Lara G A, Orellana P A and Anda E V 2008 *Phys. Rev. B* **78** 045323

[27] Trocha P, Weymann I and Barnaś J 2009 *Phys. Rev. B* **80** 165333

[28] Awschalom D D, Loss D and Samarth N 2002 *Semiconductor Spintronics and Quantum Computation* (Berlin: Springer)

[29] Park H, Park J, Lim A K L, Anderson E H, Alivisatos A P and McEuen P L 2000 *Nature* **407** 57

[30] Mitra A, Aleiner I and Millis A J 2004 *Phys. Rev. B* **69** 245302

[31] Dong B, Cui H L and Lei X L 2004 *Phys. Rev. B* **69** 205315

[32] Zazunov A, Feinberg D and Martin T 2006 *Phys. Rev. B* **73** 115405

[33] Siddiqui L, Ghosh A W and Datta S 2007 *Phys. Rev. B* **76** 085433

[34] La Magna A and Deretzis I 2007 *Phys. Rev. Lett.* **99** 136404

[35] Galperin M, Ratner M A and Nitzan A 2007 *J. Phys.: Condens. Matter* **19** 103201

[36] Ueda A and Eto M 2007 *New J. Phys.* **9** 119

[37] Galperin M, Nitzan A and Ratner M A 2008 *Phys. Rev. B* **78** 125320

[38] Weber C, Fuhrer A, Fasth C, Lindwall G, Samuelson L and Wacker A 2010 *Phys. Rev. Lett.* **104** 036801

[39] Vidmar L, Bonča J, Mierzejewski M, Prelovšek P and Trugman S A 2011 *Phys. Rev. B* **83** 134301

[40] Kim Y, Song H, Strig F, Pernau H F, Lee T and Scheer E 2011 *Phys. Rev. Lett.* **106** 196804

[41] Tagani M B and Soleimani H R 2011 *Physica B* **406** 4056

[42] Tagani M B and Soleimani H R 2012 *Phys. Scr.* **86** 035706

[43] Dong B, Cui H L, Lei X L and Horing N J M 2005 *Phy. Rev. B* **71** 045331

[44] Qin H, Holleitner A W, Eberl K and Blick R H 2001 *Phys. Rev. B* **64** 241302

[45] Lundin U and McKenzie R H 2002 *Phys. Rev. B* **66** 075303

[46] Chen Z Z, Lü R and Zhu B F 2005 *Phys. Rev. B* **71** 165324

[47] Bonča J and Trugman S A 1995 *Phys. Rev. Lett.* **75** 2566

[48] Leturcq R, Stampfer C, Inderbitzin K, Durrer L, Hierold C, Mariant E, Schultz M G, von Oppen F and Ensslin K 2009 *Nat. Phys.* **5** 327

[49] Fang T F, Sun Q F and Luo H G 2011 *Phys. Rev. B* **84** 155417

[50] Huag H and Jauho A P 1996 *Quantum Kinetics in Transport and Optics of Semiconductors* (Berlin: Springer)

[51] Langreth D C 1976 *in Linear and Nonlinear Electron Transport in Solids*, (Vol. 17) *NATO Advanced Study Institute Series B: Physics* (Ed. by Devreese J T and Van Doren V E) (New York: Plenum)